Fusion Engineering and Design 178 (2022) 113090

Contents lists available at ScienceDirect

Fusion Engineering and Design

journal homepage: www.elsevier.com/locate/fusengdes

Investigation of novel weight window methods in Serpent 2 for fusion neutronics applications

A. Valentine [*,a], R. Worrall [a], J. Leppänen [b]

[a] Culham Centre for Fusion Energy, Culham Science Centre, Abingdon Oxford, OX14 3DB, UK
[b] VTT Technical Research Centre of Finland Ltd, Kivimiehentie 3, Espoo FI-02044 VTT, Finland

ARTICLE INFO

Keywords:
Serpent
MCNP
Neutronics
Variance reduction
DEMO
SINBAD

ABSTRACT

Released in 2009, the Serpent Monte Carlo code has established itself as a highly efficient and powerful simulation code for nuclear systems analysis. Originally developed for reactor physics applications, the scope of the code now extends to coupled multi-physics simulations and photon transport. The latter has allowed adoption of the code by the fusion neutronics community following developments of a coupled neutron-photon capability in 2014 and the ability to handle complex geometry types in 2016. The code is well validated for the energy regimes and geometry types one can expect in fission reactor analysis. Over the course of recent years a benchmarking effort has been undertaken for application of the code to nuclear fusion. Compared to nuclear fission, or accelerator based applications, the underlying particle interaction phenomena differ greatly at the energies expected in a fusion reactor as well as the specific responses that are of interest. In this paper, a novel weight window generation implementation in Serpent is investigated. The applicability of this method is demonstrated for the Frascati Neutron Generator (FNG) bulk blanket and shield experiment, part of the SINBAD database, and a DEMO helium cooled pebble bed (HCPB) computational model. A comparison is performed against MCNP using weight windows generated with ADVANTG. Excellent agreement is found for the specified tallies and the significant efficiency gain using weight windows generated using both methods is comparable. A robust variance reduction method implementation is fundamental to applications to fusion neutronics and as such, this work is an important step in deployment of Serpent for this type of analysis.

1. Introduction

Radiation transport models for fusion neutronics analysis are becoming increasingly complex, placing additional demands on traditional 3D computational nuclear analysis methods using MCNP [1]. Investigations into potential alternative and complementary analysis codes and tools facilitate the evolution of neutronics analysis method development to meet requirements and further the confidence in results through multiple codes and calculation workflows. To this end, this paper builds on the motive for using Serpent 2 [2], developed at VTT Technical Research Centre of Finland, for fusion neutronics analysis.

MCNP is an established code with significant history in radiation transport problems and is considered the standard code for ITER related fusion neutronics. Complex models, such as the ITER neutronics reference model, have resulted in the MCNP geometry creation and integration process becoming increasingly time-consuming and inefficient. Significant time is required to produce a suitably simplified system model and successfully integrate it into the ITER reference model. Some of the main issues regarding the implementation of large complex universe-based models was discussed in previous work [3] with some alternative CSG and mesh-based neutronics analysis approaches, including Serpent 2, also investigated. Initial results in comparison to the conventional MCNP constructive solid geometry method have proved agreeable [4,5].

In spite of the increasing bottlenecks which scale with the complexity of the models, MCNP remains the most widely adopted particle transport code. The simple reason for its prevalence is that the code is validated to meet the complete set of fundamental requirements for the code to be applied to all fusions neutronics problems. These include: neutron and photon coupled radiation transport using point-wise cross section libraries; able to provide a geometric representation of the modelled system in all its complexity; accommodate complex plasma neutron source definitions; have parallelisation capability for deployment on high performance computer architectures; and be capable of employing

* Corresponding author.
E-mail address: alex.valentine@ukaea.uk (A. Valentine).

https://doi.org/10.1016/j.fusengdes.2022.113090
Received 11 August 2021; Received in revised form 28 February 2022; Accepted 4 March 2022
Available online 9 March 2022

acceleration techniques. A complete account of the requirements is given in Pampin et al. [6]. All but the final of these requirements have been rigorously tested for application to fusion.

There are several methods of accelerating Monte Carlo calculations using non-analogue techniques, all of which share the common purpose of increasing the likelihood that a particular particle contributes to the specified response. Detailing the various variance reduction methods is beyond the scope of this paper; instead we focus on perhaps the most commonly applied method to fusion neutronics problems, weight windows. Weight windows are a mesh based method of population control that uses splitting and Russian roulette as a means of controlling the number of histories.

For complex neutron-photon shielding problems in MCNP, ADVANTG [7], developed by Oak Ridge national laboratory has become a powerful tool for automating the generation of variance reduction parameters. Other methods [8] based on superimposed meshes involve iteratively populating the geometry over the defined mesh and generating the energy dependent weight window bounds for deep shielded regions. Both methods support a global approach for achieving uniform convergence over the region of interest. Of the above requirements listed for code deployment on real fusion problems, all but the final have been rigorously investigated since the scope of Serpent evolved to encompass nuclear fusion. An in-built routine based on the response matrix method has been introduced in Serpent for automated generation of weight windows [9]. The investigation of this novel development is the focus of this paper.

The limited number of global experiments simulating fusion-like conditions provides precious data for validation of theoretical models and underlying nuclear data. The SINBAD database, controlled and released by the NEA, contains 31 fusion related experiments that were in the most part performed over 20 years ago. The Frascati Neutron Generator (FNG) experiments performed at ENEA Frascati consist of several different geometrical mock ups irradiated with a 14 MeV neutron source. In this work, the bulk blanket and shielding experiment conducted between 1995 and 1997 is selected as a suitable experimental configuration for investigating variance reduction. The purpose of this experiment was to validate the blanket shield design for ITER, on track for first plasma in 2025.

To demonstrate application over a much larger spatial extent, an EU DEMO Helium Cooled Pebble Bed (HCPB) MCNP sector model has been used. This homogenised representation of EU DEMO includes a description of all major tokamak components up to and including the bioshield. A validation of Serpent for assessing a range of nuclear responses in-vessel has previously been reported in Valentine et al. [4]. Here, our focus extends beyond the vacuum vessel as validation of the weight window implementation in Serpent, specifically, the response in poloidal field coils (PFC) which span the poloidal extent of the ex-vessel region. In the first part of the paper, a brief summary of the variance reduction methods are presented before detailing the results from the FNG (Section 4.1) and DEMO HCPB (Section 4.2) calculations respectively. Finally we conclude our findings as well as providing important subjective guidance on future qualifications (Section 6) of Serpent for this application. The results presented herein provide demonstration of the suitability of Serpent application to complex fusion neutronics problems.

2. Methodology

MCNP version 6.2 [1] was used for benchmarking computational results with Serpent version 2.1.31 beta [10]. Because this version of the code is still under development, updates to Serpent are applied through raising a request with the development team therefore exact versions of the code may differ.

All models in this work are geometrically represented in constructive solid geometry (CSG) format. Potentially more efficient workflows using CAD based tracking are currently being investigated and are listed as an area for potential future work for improved efficiency in the neutronics workflow.

The reference nuclear data library used for neutron transport for the FNG experiment is FENDL-2.1 [11]. Dosimetry cross section libraries have been used for the activation foils, namely IRDFFv1.05 [12]. For DEMO neutron transport simulations, cross sections are taken from JEFF-3.2 [13]. The adopted photon library in all cases is MCPLIB04/84 [14].

The parametric plasma source description for DEMO was re-written as a C routine for deployment in Serpent. Serpent allows user defined source routines and the parametric plasma source is called as such. The analysis assumes 1998 MW thermal power giving a normalisation equal to 7.094×10^{20} neutrons s^{-1}.

Source duplication was also required for the FNG experiment which has been written as a routine in MCNP. A list of starting source particles with position, energy, direction and weight has been generated in an MCNP simulation and a routine produced to read this in to Serpent. All calculations were performed to 10^8 neutron histories using an internal UKAEA Intel Xeon E5-2665 computing cluster.

3. Variance reduction methods

A very detailed theoretical background on the variance reduction scheme and its evolution in Serpent can be found in Leppänen [9]. The first implementation of variance reduction was introduced in Serpent 2.1.27 in 2017. Aside from the built in weight window generator, it is also possible to read in a weight window generated by ADVANTG in MCNP's WWINP format. In this method, an identical weight window file can be read by both MCNP and Serpent however the focus here is on the native Serpent weight window generation method.

Weight windows are one example of a broader category of so called population control methods. The other common variance reduction technique under this subset of methods is geometry splitting with Russian roulette. At a basic level, this involves the concept of assigning cell based importances which can be input by the user in order to roulette and split the particles, such that 'important particles are tracked more frequently through the geometry. Each has their advantages and disadvantages depending on the particular application. It has in more recent years become common to combine the two methods which is straightforward given that they are implicitly inversely proportional to each other a region of high importance will imply the weights of the particles are low and thus the lower bound of the weight window will be low.

Each event is assigned an importance and the particle population is encouraged to migrate towards regions of higher importance using the weight window mesh. Serpent uses the response matrix method to the particle transport problem in order to derive importances to a discretised geometry space as defined on a user defined cartesian or cylindrical mesh.

The most elaborate development of the Serpent weight window generator is its adaptive mesh capability. If this option is selected, the voxels which comprise the weight window mesh can be split recursively to the point when a user supplied density criterion is satisfied. The implementation is based on an Octree-type method where a cartesian mesh voxel represents a node of the data structure, and as such is split recursively into 8 sub-nodes until the density criterion is satisfied. The use of an adaptive mesh is well suited for deep shielding problems where there are regions of heavy shielding and large regions of void i.e. a typical tokamak. Where there is a high-density medium, with which steep importance gradients are present, a finer mesh resolution is required to obtain an optimal importance mesh. Keeping the mesh coarse in void regions can save significant computing resource. The recursive splitting of cells (Fig. 1) is an inexpensive computational operation performed by passing random histories through the geometry prior to starting the transport simulation.

In this scheme, the calculation effectively becomes a three step

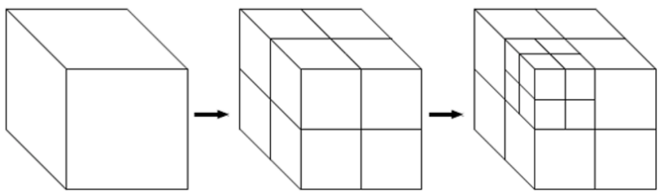

Fig. 1. Illustration of the recursive splitting which Serpent performs to the spatial mesh.

problem whereby the user first runs the global variance reduction (GVR) iterations, then optimises the mesh for a specific detector and finally the calculation is run with the optimised mesh. One computational benefit of this methodology is that all of these steps can be combined into a single calculation. The importances underpinning the weight window as described in the previous section are derived using an adjoint transport calculation, the solution of which is the importance function or importance map. In Serpent, the adjoint solution is obtained from a response matrix method based solver, which effectively tracks neutron currents backwards through the mesh. The coupling coefficients, however, are obtained from a forward Monte Carlo simulation. Conversely, this is typically done deterministically, as in ADVANTG, which uses the Denovo [15] discrete ordinates code to derive the adjoint fluxes.

ADVANTG uniformly converges tallies for arbitrary single responses, or across the entire global problem domain such as through the convergence of results in individual voxels of a mesh tally. Once the discrete ordinates calculation (including mapping of the materials on to the spatial mesh) is complete over the MCNP geometry, there are two methods implemented in ADVANTG, namely CADIS [16] and FW-CADIS [17], that are used to derive the weight window parameters. The CADIS method is developed for individual tally responses, while FW-CADIS can be multiple individual tallies or mesh tallies. The output from ADVANTG are the weight window lower bounds in MCNP weight window input file format (WWINP). We have investigated weight windows optimised for both a targeted single response detector and multiple detectors in this work. The comparison in all cases is between MCNP using a WWINP file generated through ADVANTG, and Serpent using its built in methods to produce a weight window for the equivalent geometry and source terms.

4. Results and discussion

4.1. FNG bulk blanket and shield experiment

The geometry of the set up has been described in MCNP and the input file distributed with SINBAD. This has been converted to Serpent using a python script which automates the conversion between several Monte Carlo codes, CSG2CSG [18]. A CAD representation of the geometry, obtained through inversion to.sat file format with SuperMC [19], is shown in Fig. 2. The mock up consists of a geometrical description of the first wall, blanket, vacuum vessel and the toroidal field coils. The materials were selected to replicate the inboard ITER in-vessel components at the time of the experiment. The front wall is a 1 cm thick layer of copper. The body of the blanket and vacuum vessel is described by 316 stainless steel and perspex ($C_5O_2H_8$) sandwich of 94.26 cm thickness. The perspex was chosen to model water. A smaller block at the rear of the mock-up comprises alternating layers of 2 cm thick copper and 316 stainless steel to represent a toroidal field coil.

In the experiment, the reaction rates for a series of 1.8 cm diameter activation foils at increasing distance from the source were measured using a set of calibrated High Purity Germanium (HPGe) detectors. In this work, we have computationally determined the reaction rate in gold for the reaction ^{197}Au(n,g).

With increasing distance from the source, the relative error on the calculated response for each of the foil cells captured through MCNP F4 tallies increases beyond a depth of 17.15 cm in the analogue scheme as the level of shielding between the target and source increases. The foil at the rear of the blanket/vacuum vessel is located at a distance of $\simeq$ 1 m from the source. The experimentally determined reaction rates and values calculated in Serpent with an analogue simulation are given in Table 1.

The reaction rates are determined using IRDFF v1.05 - a calculation was repeated using the LLDOS [20] library and the deviation from

Table 1
Measured and Serpent calculated reaction rates for ^{197}Au(n,g) in and analogue neutron transport simulation. Reactions are given in units of number of reactions per unit volume/(10^{24}*source neutrons).

Depth (cm)	Measured	Calculated	C/E
3.43	6.37E – 03 (0.04)	5.97E – 03 (0.07)	0.94
10.32	9.72E – 03 (0.04)	9.47E – 03 (0.05)	0.97
17.15	5.50E – 03 (0.04)	5.41E – 03 (0.07)	0.98
23.95	2.44E – 03 (0.04)	2.62E – 03 (0.10)	1.07
30.80	9.47E – 03 (0.045)	7.55E – 04 (0.17)	0.80
41.85	1.65E – 04 (0.045)	(>30%)	
53.80	3.76E – 05 (0.05)	(>30%)	
60.55	1.71E – 05 (0.05)	(>30%)	
67.40	6.82E – 06 (0.05)	(>30%)	
74.40	2.68E – 06 (0.055)	(>30%)	
81.10	1.12E – 06 (0.055)	(>30%)	
87.75	3.66E – 07 (0.065)	(>30%)	
92.15	1.71E – 07 (0.085)	(>30%)	

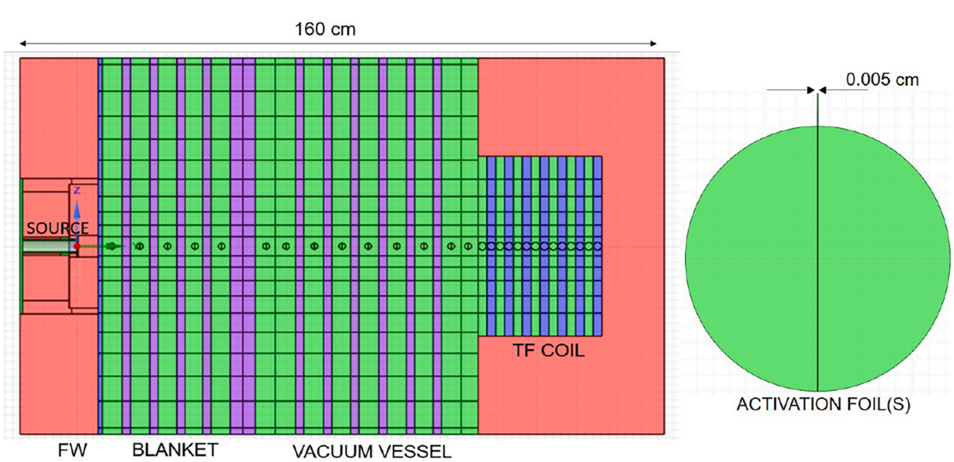

Fig. 2. FNG bulk blanket and shielding experiment geometry at $x = 0$. The activation foils can be seen through the centre of the blanket encapsulated in a spherical shell (right).

experimental data found to be on average a factor of 2 between the libraries. Significant updates, including for radiative capture in Au were made. Prior to detailing the application of variance reduction in this problem it should be noted that for this relatively simple geometry, the solution of increasing the number of particle histories is feasible as the computational run time does not become a major bottleneck. This is of course subject to resource, and is nonetheless a less elegant route to statistical convergence. Where possible, a universal approach should be adopted.

A weight window has been generated in Serpent using a GVR approach. A Cartesian mesh was defined to cover all geometry space with no energy binning. The mesh is optimized to uniformly populate the entire geometry. The calculation proceeds iteratively; it was found that after 3 iterations, cell tallies in individual foils through the geometry had sufficiently converged. Further iterations provided no obvious gain in efficiency. Note that particle splitting can cause significant variation in the length of simulated histories resulting in fluctuation of CPU usage. The 'set bala' option in Serpent was called in all simulations to mitigate this problem.

Using ADVANTG, an equivalent global scheme was attempted using a mesh covering the entire geometry, however, this was not suitable for individual foil responses which vary from close proximity to the source to highly shielded regions. Instead, the cell tallies for all activation foils were listed as the targeted responses and a weight window generated in the FW-CADIS scheme. In line with Serpent, a 5 × 5 × 5 cm^3 mesh was defined for the spatial mesh. In both cases, the time taken to produce the weight windows was on the order of seconds. The statistical error over the extent of the geometry in each of the three simulation cases is shown in Fig. 3. This serves as demonstration of the power of these methods in automating the sequence of variance reduction parameter generation. One may expect that using methods such as the iterative weigh window generator to MCNP could take several hours of 'fine-tuning' to produce a suitable weight window.

The targeted approach taken in ADVANTG is evident in Fig. 3c whereby the error is reduced along the axis (foil locations) of the experiment. In Serpent, use of a global approach achieves uniform population of the entire geometry and hence a relative error across over 96% of the voxels of less than 5%. The time taken to produce the weight window in Serpent was 23 CPU minutes, compared to 8 CPU minutes for the ADVANTG weight window. The Serpent transport simulation took 192 CPU minutes compared to 272 CPU minutes for MCNP. A comparison of the calculated reaction rates and the experimental data is shown in Fig. 4. For the same number of simulated histories, a result has been obtained in all 14 of the activation foils with the maximum uncertainty on the foil furthest from the source equal to 11.5% in Serpent and 21.2% in MCNP.

MCNP and Serpent are in agreement within the bounds of uncertainty for all foils other than the final foil with associated largest uncertainty. For this foil, a weight window optimised for this specific response could be generated in future analysis to reduce the statistical error. In any case, both results are in good agreement with the experimental data given the uncertainty.

It is also possible to apply Serpent to target individual foil responses. In this case, only the targeted result remains valid as contributions to other responses may have been 'killed' due the bias in the simulation. For more heavily shielded regions, it is however necessary to firstly populate the geometry in the global approach otherwise particles may fail to reach the target and the response matrix solver will not run. This approach of applying global variance reduction and subsequently targeting the response of interest is the most effective method in Serpent for deep shielding problems as demonstrated in Section 4.2

4.2. DEMO HCPB

The DEMO HCPB model was produced taking the MCNP reference model for EUROfusion neutronics analysis and using CSG2CSG to produce the Serpent file (Fig. 5). The geometry is plotted using the pysss2 python package [21], a fully interactive Serpent geometry visualisation tool. The model represents a 10° sector of the tokamak with reflecting planes on the lateral bounds of the sector to approximate toroidal symmetry. Manual modifications have been performed largely related to the blanket modules described using lattices. This is one geometry feature which is implemented significantly differently in Serpent. Following validation of the geometry conversion process, coupled neutron-photon transport simulations were performed to 10^8 neutron histories.

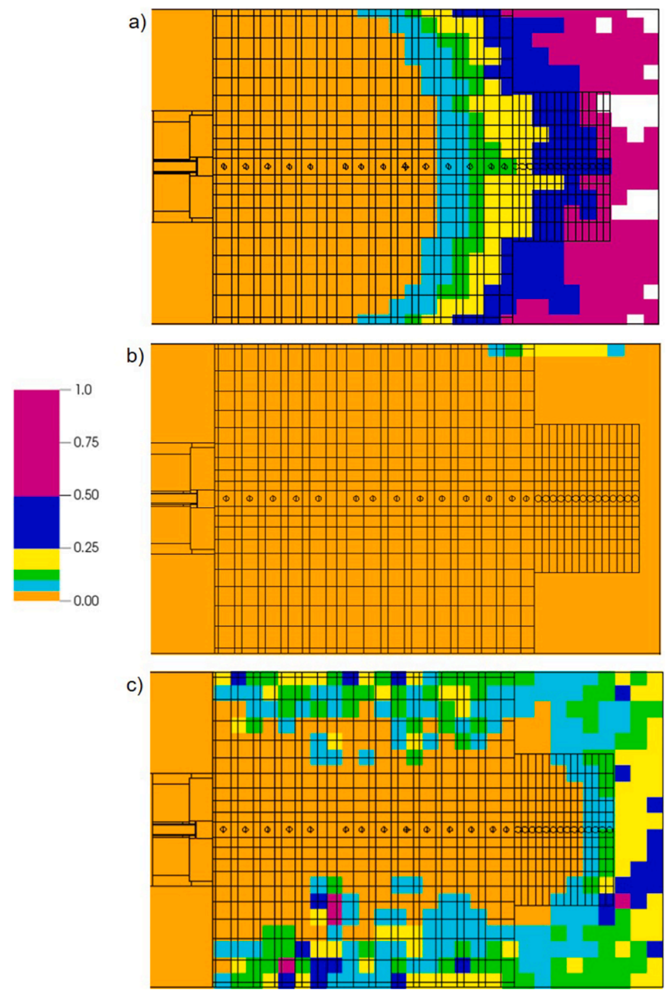

Fig. 3. Map of the relative statistical error in (a) Serpent analogue (b) Serpent generated weight window and (c) MCNP + ADVANTG weight window.

A weight window has been generated in Serpent using the built in solver based on 3 iterations. Here the adaptive mesh option was used - the cells of the overlaid 10 × 10 × 10 cm^3 voxel Cartesian mesh are recursively split until the density criterion is met. ADVANTG with the global spatial treatment was also used with 10 cm spatial resolution, extending over the extent of the geometry. The neutron flux and associated statistical error calculated on a 5 cm resolution mesh is shown in Fig. 6.

Very good agreement is found between the calculated values of neutron flux in the mesh voxels. The statistical error is below 5% across the majority of the model and for these voxels, the maximum % deviation in neutron flux in any one voxel is 4% with all data points lying in the bounds of uncertainty. Only in the deepest shielded regions such as the vacuum vessel and center of the TF coil winding pack does the error exceed 50%, results for which the MCNP user manual instructs should be ignored. This demonstrates the efficiency of the Serpent weight window

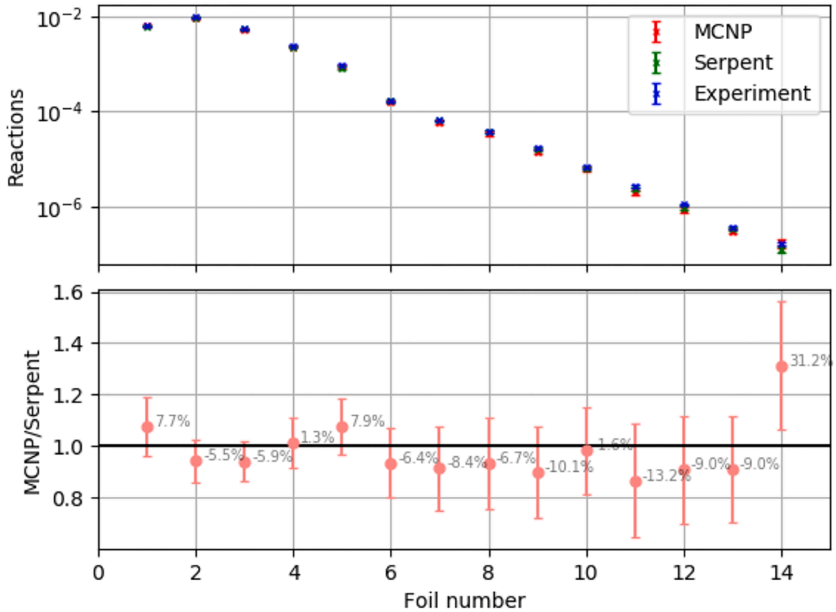

Fig. 4. Comparison of Serpent, MCNP and experimental evaluations of reaction rates through the FNG mock up. Simulations are performed in the non-analog scheme. The data is given in units of number of reactions/(10^{24}*source neutrons). The foil numbers starting at 1 closest to the source, increasing sequentially corresponding to increasing distance from the source.

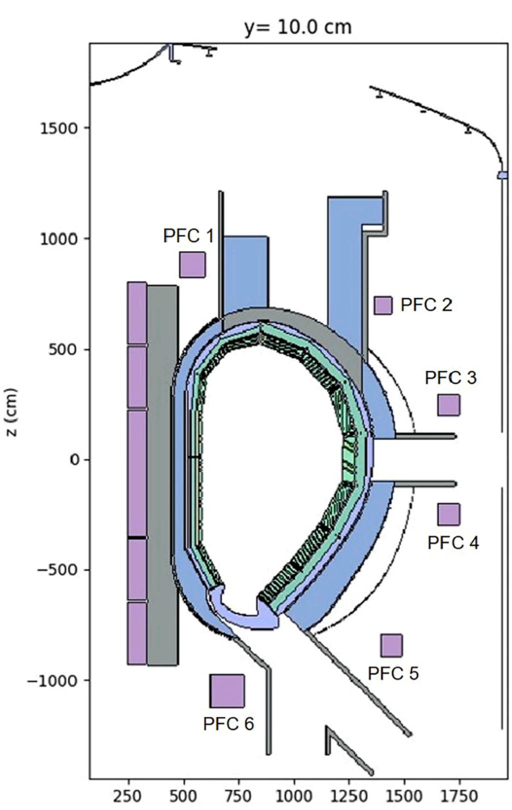

Fig. 5. DEMO HCPB Serpent geometry at $Y = 10$ cm. Each of the poloidal field coils are labelled.

generator in achieving global uniform convergence across the entire problem space in a complex fusion reactor problem.

The figure of merit (FoM) is one of ten statistical tests reported as a standard output in MCNP. This gives an indication of the computational efficiency through factoring the run time and the magnitude of uncertainty as FOM=$\frac{1}{\sigma^2 T}$, where σ is the variance and T the computing time. For each of the PFC, 1–6, which are located around the ex vessel region the ratio of the FOM between the analogue and calculation with applied weight window is given in Table 2. The ratio of the FOM gives an indication of the increase in efficiency.

Of the other statistical tests reported by MCNP, in the analogue simulation, 7 out of 10 were passed. With the applied weight window, 8 statistical tests were reported to pass. The decrease in variance of the variance and the rate of its decrease both reported failure in this case. While these tests provide an extremely valuable metric when applying variance reduction methods given that we are introducing a bias into the simulation. However, not all test failures are significant. When examining results, it is ultimately at the users discretion to provide the ultimate judgement on tally convergence. In this case, the increase observed is deemed to be insignificant.

Typically, tally convergence for specific results of interest is required. Of the 6 coils, PFC 1 is the most heavily shielded due to its positioning relative to port openings which provide a natural streaming path for neutrons. A weight window optimised for this particular coil was produced in Serpent. For this type of problem, it was necessary to first run a GVR calculation, again, with an adaptive mesh, followed by further iterations to produce a mesh optimised for the response in PFC 1.

The weight window was checked to be performing as expected by plotting a map of the neutron importances which is calculated by Serpent as a solution to the adjoint transport problem. Serpent automatically generates these plots over a user defined logarithmic scale. Trials using weight windows optimised for PFC 4 and 6 are also shown as demonstration of the effectiveness of this method for targeting different regions of the problem geometry space (Fig. 7). In each case, it is evident that the weight window is correctly targeting the specified response. In terms of the computational efficiency, for PFC 1, the ratio in FOM between the non-analogue and analogue calculation is 67, 720 in PFC 4 and as high as 1043 in PFC 6.

In ADVANTG, a single calculation was performed with the specified target response using a cell tally in MCNP. The neutron flux in 175 (VITAMIN-J) energy groups for PFC 1 is shown in Fig. 8. No energy binning on the tallied response was applied in calculating the weight window in ADVANTG or Serpent.

In general there is good agreement for the 175 energy groups. 129

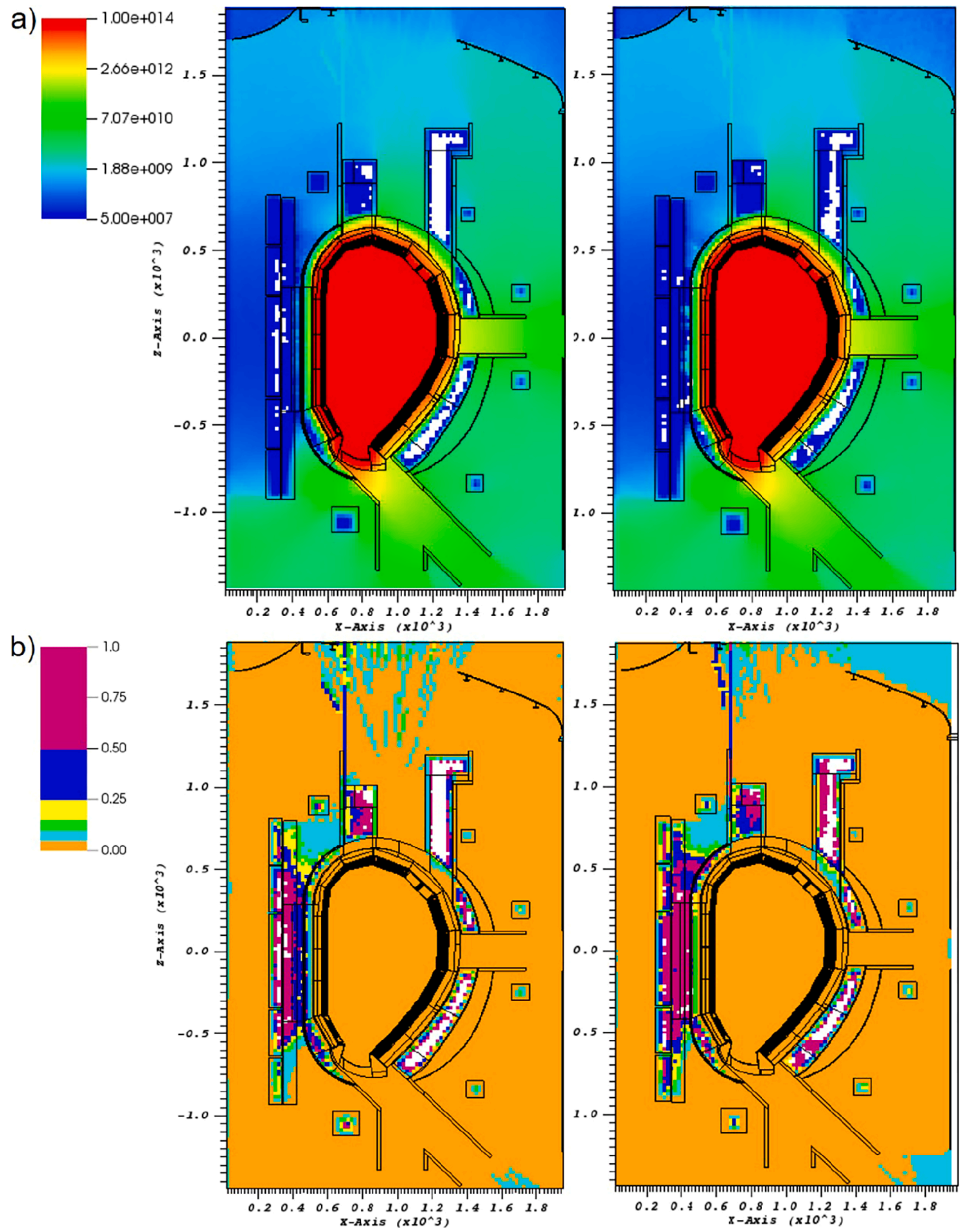

Fig. 6. (a) Neutron flux (n cm^{-2} s^{-1}) for MCNP + ADVANTG (left) and Serpent (right) using a weight window generated in the global approach (b) Associated relative error map. White represents zero response.

Table 2
Calculated neutron flux and associated statistical error in PFC 1 to 6 for the analogue and non-analogue calculations.

	Neutron flux (n cm^{-2} s^{-1})			
	Coil	Analogue	Non-analogue	FOM ratio
MCNP	1	3.18E14 (0.43)	3.78E14(0.017)	69
	2	5.32E15(0.12)	4.70E15(0.002)	139
	3	2.59E16(0.06)	2.47E16(0.002)	60
	4	1.73E16(0.08)	2.67E16(0.002)	57
	5	1.73E16(0.08)	1.60E16(0.002)	121
	6	6.68E16(0.04)	6.52E16(0.002)	39
Serpent	1	4.27E14(0.24)	3.65E14(0.02)	306
	2	4.09E15(0.08)	4.57E15(0.004)	1041
	3	2.49E16(0.04)	2.40E16(0.003)	456
	4	2.58E16(0.03)	2.60E16(0.003)	348
	5	1.59E16(0.04)	1.55E16(0.002)	735
	6	6.09E16(0.02)	6.34E16(0.002)	515

points, covering 74% of the data set lie within 2σ uncertainty it is noticeable that many of the results with > 2σ lie in the low energy region owing to the very small uncertainties (less than 0.5%) on these results. The maximum deviation reported below 10^{-2} MeV is 5%. At higher energies there are some more significant discrepancies with large uncertainties. These occur above the fusion peak as the adopted VITAMIN-J group structure extends up to 19.6 MeV. In general, the difference is likely due to differences in tallying reaction rates between the two codes. MCNP uses a track length estimator (TLE) while Serpent uses a collision flux estimator (CFE). The former is generally superior because tracks are scored each time a particle crosses a given region even if no collisions occur. In Serpent, the TLE estimator can be invoked through the 'dtl' option, or otherwise, the mean distance for scoring the collision flux estimator can be decreased with the 'set cfe' option. It is expected based on the results in Leppänen [22] that this would improve the comparison presented here and further investigation should be conducted.

The increase in computational efficiency relative to the analogue

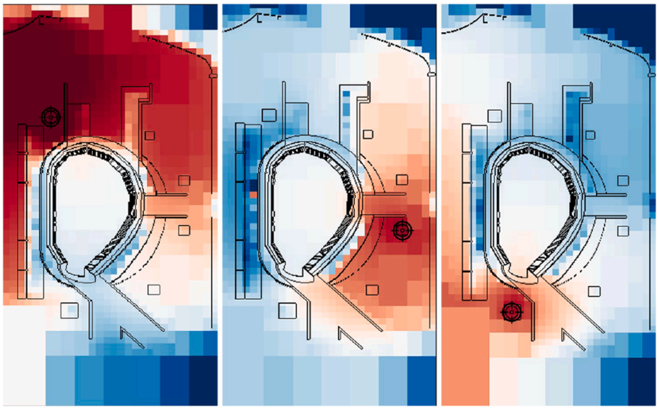

Fig. 7. Maps of the neutron importances using a logarithmic scale from 1×10^{-5} to 1×10^{5}. WW optimised for PFC 1 (left), PFC 4 (centre) and PFC 6 (right).

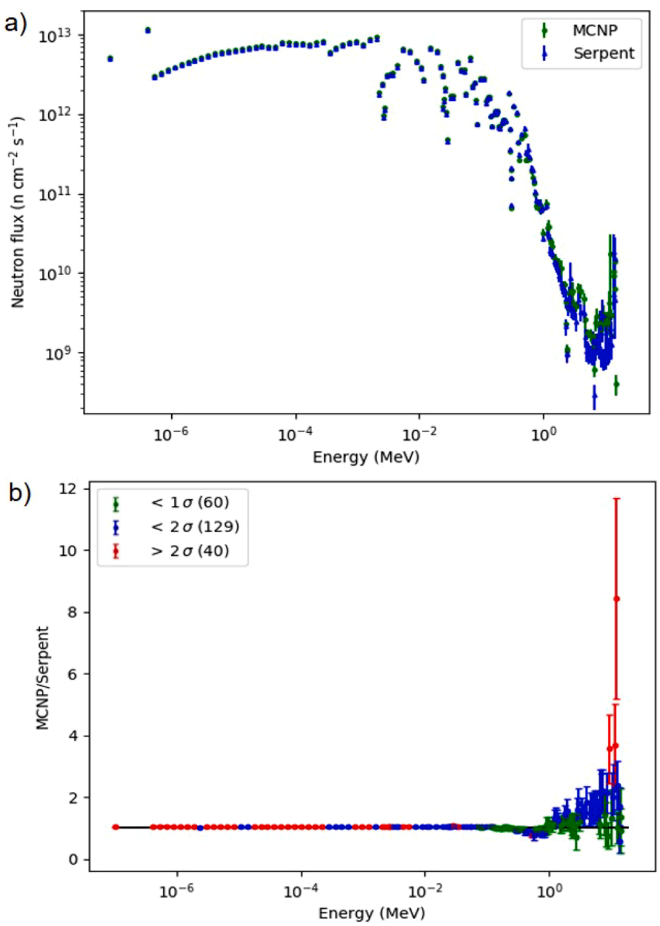

Fig. 8. (a) Comparison of the Serpent and MCNP calculated neutron flux in 175 energy groups at PFC 1. (b) Ratio of results showing the data points lying withing 2σ uncertainty.

simulation is clear from Table 2. The factor increase in the FoM is the important quantity reported here. Throughout this work, the emphasis is in comparison of the analogue and non-analogue simulations of each respective code. The importance of the cross code comparison is in validation of the absolute values. A direct comparison is more involved because of the distinct differences between the two methods. Each method has a set of parameters which are unique to the code and have been selected based on optimising the weight window (see Leppänen et al. [23] for more information on Serpent). On this basis we summarise that both methods provide an automated means of generating weight windows on the time scale of hours for complex fusion geometries. While a non-specific conclusion, the methods of variance reduction predating these advancements could commonly involve iterations spanning several days.

5. Conclusion

The novel variance reduction methods in Serpent have been investigated for application to fusion relevant analysis. We have demonstrated that the recent developments to the code provide an efficient and potentially robust means of generating weight windows through its built in response matrix method-based solver. The method has been applied to the FNG bulk blanket and shielding experiment from the SINBAD database, and a computational model of EU DEMO HCPB, both geometrically diverse applications in complexity and scale.

The capability to achieve uniform convergence over the global space of the problem has been demonstrated in both cases. For the FNG benchmark, the reaction rate in a series of activation foils positioned through the geometry resembling the ITER inboard shielding is calculated within the bounds of experimental uncertainty across all foils with the applied weight windows. This was extended to converging the results for individual poloidal field coils in DEMO HCPB, where the adaptive mesh option using a global and subsequent simulation optimising it for a targeted response proved to be most optimal. The results demonstrated very good agreement for individual cell responses with less than 3% deviation to the response calculated using MCNP and a global weight window generated in ADVANTG. In the case of targeting the response of PFC 1, 83% of the results lie within 3 σ uncertainty between Serpent and MCNP.

MCNP remains, at the time of writing, the most widely applied Monte Carlo code for fusion neutronics analysis. In recent years there is a growing shift to using alternative, emerging transport codes, as their capabilities are extended to the scope of fusion neutronics. This is in line with the increasing complexity of radiation transport models as the level of model fidelity tangentially approaches that of the constructed model. Serpent is a forerunner of these alternative codes following the development of key features of the code needed for application to this field. For deployment on problems typical of current fusion nuclear analysis, variance reduction remained until 2017, the only major omission from the code. In this paper, the results serve as demonstration of the capability of Serpent to perform as well as ADVANTG for heavily shielded responses, holding great promise for the code to be extended to the most complex of practical applications.

6. Future work

Given the demonstrated capability of Serpent for fusion neutronics, it is strongly recommended that continued qualification of the code in this field is undertaken. One area in particular that should be investigated is the use of STL geometries for particle transport. This is a potentially much more robust workflow eliminating one of the major bottlenecks associated with CAD model preparation. The built in weight window generator is also applicable to this geometry type. Many of the more recent developments in Serpent have focused on improvements to the handling of STLs.

Serpent has a built in depletion solver which can be used to produce a decay gamma source. Some initial applications of this to ITER analysis has proven promising [24]. MCR2S, a code developed at UKAEA that uses the rigorous two step method for assessment of decay fields has recently been extended to couple the transport calculation performed in Serpent [25]. It is recommended that a comparison is performed between this and the built in methods in Serpent.

CRediT authorship contribution statement

A. Valentine: Conceptualization, Investigation, Formal analysis, Software, Validation, Supervision, Visualization, Writing – original draft, Writing – review & editing. **R. Worrall:** Formal analysis, Investigation, Validation, Visualization, Writing – review & editing. **J. Leppänen:** Methodology, Software, Writing – review & editing.

Declaration of Competing Interest

The authors declare that they have no known competing financial interests or personal relationships that could have appeared to influence the work reported in this paper.

Acknowledgements

This work has been carried out within the framework of the EUROfusion Consortium and has received funding from the Euratom research and training programme 2014–2018 and 2019–2020 under grant agreement no. 633053. The views and opinions expressed herein do not necessarily reflect those of the European Commission. Funding has also been provided through RCUK [grant number EP/T012250/1]. To obtain further information on the data and models underlying this paper please contact PublicationsManager@ukaea.uk. The views and opinions expressed herein do not necessarily reflect those of the European Commission.

References

[1] C.J. Werner, J. Armstrong, F.B. Brown, J.S. Bull, L. Casswell, L.J. Cox, D. Dixon, R. A. Forster, J.T. Goorley, H.G. Hughes, J. Favorite, R. Martz, S.G. Mashnik, M. E. Rising, C. Solomon, A. Sood, J.E. Sweezy, C.J. Werner, A. Zukaitis, C. Anderson, J.S. Elson, J.W. Durkee, R.C. Johns, G.W. McKinney, G.E. McMath, J.S. Hendricks, D.B. Pelowitz, R.E. Prael, T.E. Booth, M.R. James, M.L. Fensin, T.A. Wilcox, B. C. Kiedrowski, MCNP User's Manual Code Version 6.2, Los Alamos National Laboratory, 2017.

[2] J. Leppänen, et al., The Serpent Monte Carlo code: status, development and applications in 2013, Ann. Nucl. Energy (2015).

[3] A. Turner, Investigations into alternative radiation transport codes for ITER neutronics analysis, Trans. Am. Nucl. Soc. 116 (17) (2017) 251–254.

[4] A. Valentine, B. Colling, R. Worrall, J. Lepp, Benchmarking of the Serpent 2 Monte Carlo code for fusion neutronics applications. PHYSOR 2020 Conference Proceedings, 2020.

[5] A. Turner, A. Burns, B. Colling, J. Leppänen, Applications of Serpent 2 Monte Carlo code to ITER neutronics analysis, Fusion Sci. Technol. 74 (4) (2018) 315–320, https://doi.org/10.1080/15361055.2018.1489660.

[6] R. Pampin, A. Davis, J. Izquierdo, D. Leichtle, M.J. Loughlin, J. Sanz, A. Turner, R. Villari, P.P.H. Wilson, Developments and needs in nuclear analysis of fusion technology, Fusion Eng. Des. 88 (6–8) (2013) 454–460, https://doi.org/10.1016/j.fusengdes.2013.03.049.

[7] S.W. Mosher, S.R. Johnson, A.M. Bevill, A.M. Ibrahim, C.R. Daily, T.M. Evans, J.C. Wagner, J.O. Johnson, R.E. Grove, ADVANTG: An Automated Variance Reduction Parameter Generator, 2015.

[8] A. Davis, A. Turner, Application of novel global variance reduction methods to fusion radiation transport problems. International Conference on Mathematics and Computational Methods Applied to Nuclear Science and Engineering, 2011.

[9] J. Leppänen, Response matrix method-based importance solver and variance reduction scheme in the Serpent 2 Monte Carlo code, Nucl. Technol. (2019) 1–17, https://doi.org/10.1080/00295450.2019.1603710.

[10] J. Leppänen, M. Pusa, T. Viitanen, V. Valtavirta, T. Kaltiaisenaho, The Serpent Monte Carlo code: status, development and applications in 2013, Ann. Nucl. Energy 82 (2015) 142–150.

[11] D.L. Aldama, A. Trkov, FENDL-2.1: Evaluated nuclear data library for fusion applications, INDC(NDS)-467 (2004).

[12] E.M. Zsolnay, R. Capote, H.K. Nolthenius, A. Trkov, Summary description of the new international reactor dosimetry and fusion file (IRDFF release 1.0), Technial report INDC(NDS)-0616(2012).

[13] NEA, The JEFF-3.2 evaluated data library - neutron data(2014).

[14] M.C. White, Further Notes on MCPLIB03/04 and New MCPLIB63/84 Compton Broadening Data for all Versions of MCNP5. LA-UR-12-00018, Los Alamos National Laboratory, 2012.

[15] T.M. Evans, A.S. Stafford, R.N. Slaybaugh, K.T. Clarno, Denovo: a new three-dimensional parallel discrete ordinates code in SCALE, Nucl. Technol. 171 (2) (2010) 171–200, https://doi.org/10.13182/NT171-171.

[16] J.C. Wagner, A. Haghighat, Automated variance reduction of Monte Carlo shielding calculations using the discrete ordinates adjoint function, Nucl. Sci. Eng. 128 (2) (1998) 186–208, https://doi.org/10.13182/NSE98-2.

[17] J.C. Wagner, D.E. Peplow, S.W. Mosher, FW-CADIS method for global and regional variance reduction of Monte Carlo radiation transport calculations, Nucl. Sci. Eng. 176 (1) (2014) 37–57, https://doi.org/10.13182/NSE12-33.

[18] A. Davis, CSG2CSG, 2020, (https://github.com/makeclean/csg2csg).

[19] Y. Wu, J. Song, H. Zheng, G. Sun, L. Hao, P. Long, L. Hu, CAD-based Monte Carlo program for integrated simulation of nuclear system SuperMC, Ann. Nucl. Energy (2015), https://doi.org/10.1016/j.anucene.2014.08.058.

[20] R.C. Little, R.E. Seamon, Dosimetry/Activation Cross Sections for MCNP. LA-UR-98-549, Los Alamos National Laboratory, 1984.

[21] S. Äkäslompolo, pysss2, 2020, (https://pypi.org/project/pysss2/).

[22] J. Leppänen, On the use of delta-tracking and the collision flux estimator in the Serpent 2 Monte Carlo particle transport code, Nucl. Technol. (2017) 161–167, https://doi.org/10.1016/j.anucene.2017.03.006.

[23] J. Leppänen, et al., 2018, (http://serpent.vtt.fi/mediawiki/index.php/Variance_reduction).

[24] J. Leppänen, T. Kaltiaisenaho, Expanding the use of Serpent 2 to fusion applications: shut-down dose rate calculations. Physics of Reactors 2016, PHYSOR 2016: Unifying Theory and Experiments in the 21st Century vol. 5, 2016, pp. 2872–2883.

[25] T. Eade, B. Colling, J. Naish, L.W. Packer, A. Valentine, Shutdown dose rate benchmarking using modern particle transport codes, Nucl. Fusion 60 (5) (2020), https://doi.org/10.1088/1741-4326/ab8181.